International Research Journal of Innovations in Engineering and Technology (IRJIET)

ISSN (online): 2581-3048
Volume 9, Issue 8, pp 96-106, August-2025
https://doi.org/10.47001/IRJIET/2025.908013

Adaptive Uplink-Downlink Resource Partitioning for CLI Mitigation in 5G HetNets with Dynamic-TDD

[1]Praise Igochi Onu, [2]Bourdillon O. Omijeh

[1,2]Department of Electrical/Electronic Engineering, University of Port Harcourt, Nigeria
Authors E-mail: [1]praise.onu@uniport.edu.ng, [2]bourdillon.omijeh@uniport.edu.ng

Abstract **- Advanced duplexing techniques are now required to ensure effective use of spectrum resources in 5G and beyond networks due to the exponential growth in mobile traffic and device connectivity. Unlike static-TDD, which uses fixed configurations, dynamic-TDD allows for flexibility in adjusting UL and DL sub-frame allocations to real-time traffic demands. But cross-link interference (CLI), especially DL-to-UL interference from high-power base station transmissions, poses a serious limitation to D-TDD systems. The improved interference mitigation framework presented in this paper suppresses CLI while optimizing coverage probability by combining adaptive 3D beamforming, fractional power control (FPC), and a multi-tier heterogeneous network model. The interference-to-signal ratio (ISR), path-loss propagation, and SINR coverage probability were analytically formulated and assessed under various FPC values (k = 0–1) and path loss exponents (2b = 2.5, 3.5). Based on simulation results, the suggested model significantly outperforms the traditional system, improving the DL coverage probability by up to 30% and the UL coverage probability by more than 53%. With considerable benefits for cell-edge users, the results show that uplink interference mitigation is more successful because user equipment has a lower transmit power than base stations. These results demonstrate the effectiveness of real-time interference-aware resource allocation and adaptive beamforming as scalable approaches for upcoming ultra-dense D-TDD deployments.**

Keywords: cross-link interference, dynamic-TDD, 3D beamforming, HetNet, static-TDD.

I. INTRODUCTION

A number of requirements, i.e., high data rates, high spectral efficiency, and low latency, has become progressively stringent for the development and deployment of future wireless communication systems as a result of the recent exponential growth in data traffic and mobile devices [1]. To accommodate the rising amount of data from mobiles and to address various kinds of users, 5G's radio interface or 5G New Radio (NR), has been made very flexible by utilizing some key technologies. Three of such technologies referred to with 5G are: enhanced mobile broadband (eMBB), massive machine-type communication (mMTC), and ultra-reliable and low-latency communication (URLLC)[2].Augmented network flexibility, enhanced reaction time, and enhanced data throughput are all supported by 5G, which has made rapid internet connectivity more practical. Virtual reality, enhanced online video, and developments in autonomous vehicles are a few of the new technologies that will be made possible now that 5G is mainstream. 5G uses the latest-generation NodeB (gNodeB) radio equipment. This is the cellular network node that links the packet core developing (EPC) with mobiles users or mobile user equipment (UE). 5G gNodeB is comparable to the conventional cellular network base station (BS) which is the radio access network (RAN). In order for wireless communication to take place over the 5G network, the gNB directly connects with user equipment (UE).

In a method to reduce the interference experienced during uplink and downlink transmission, 5G NR relies on time division duplex (TDD) rather than frequency division duplex (FDD), which has paired frequency channels with a guard band. Time division duplexing (TDD) employs the same frequency band for transmission by alternating downlink and uplink sub-frames as per time slots. Consequently, there is more flexibility in resource management and more variation in frequency. Channel reciprocity is another excellent feature of TDD mode. With this, the transmitter is able to use the estimated return link channel to estimate the outward link channel. Because of these features, TDD is more suited than FDD for features of 5G NR like 3D beam forming, massive MIMO, and small cell deployments in mm Wave frequency bands. 5G NR facilitates dynamic TDD (D-TDD) to improve the network's performance with greater duplexing flexibility[3]. There exist two modes for utilizing TDD: the dynamic mode and the static mode.

Under conventional Static-TDD (S-TDD) mode, all radio cells in a common frequency channel must have coordinated uplink/downlink sub-frame configurations among themselves. Depending on the existing traffic conditions, D-TDD permits non-synchronized sub-frame configurations in every cell. The cells use time domain partitioning to assign uplink and downlink sub-frames so that S-TDD transmissions do not overlap. The ratio of assigned sub-frames in each direction is determined for each utilizing average traffic statistics over a time interval. One usual issue of dense heterogeneous deployment is traffic imbalance between downlink and uplink

International Research Journal of Innovations in Engineering and Technology (IRJIET)

ISSN (online): 2581-3048

Volume 9, Issue 8, pp 96-106, August-2025

https://doi.org/10.47001/IRJIET/2025.908013

directions. Dynamic-TDD (D-TDD) tries to resolve this. Depending on real traffic conditions, this is more flexible and has better resource utilization. D-TDD is a type of TDD that varies the time of uplink and downlink transmission as per the current traffic. Variable traffic distribution diagrams (D-TDD) grant unique sub-frame structures to every cell.

As a result of this, synchronization is avoided, with the fact that there is better adaption of traffic. The only severe limitation of the technology is the substantial amount of interference that affects the uplink and downlink broadcasts. Thus, there are two interferences occurrence: downlink-to-uplink (whereby the downlink signal of an adjacent cell overlaps the uplink desired signal of the cell of interest) and uplink-to-downlink (whereby the downlink signal of an adjacent cell overlaps the uplink signal received by a mobile user within the cell of interest). Figure 1.1 shows the Cross-Link Interference (CLI) phenomenon. Interference between the adjacent BSs' downlink signals and the serving cell UEs' uplink signals is possible during uplink transmission, a scenario known as DL-to-UL Interference (also referred to as BS-to-BS interference). In addition, as depicted in figure 1.1, locally transmitting cells might experience uplink to downlink interference when an adjacent cell UE's uplink signal interferes with the downlink signal of the serving cell BS.

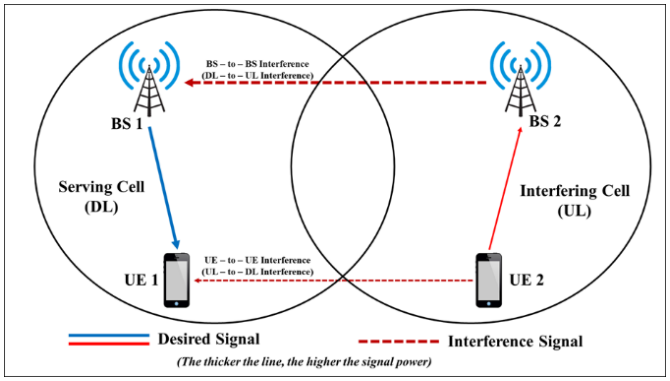

Figure 1: D-TDD Systems Cross-Link Interference

II. LITERATURE REVIEW

1. S-TDD and D-TDD

Time Division Duplexing (TDD) operates through two main modes known as Static-TDD (S-TDD) and Dynamic-TDD (D-TDD) which serve as essential duplexing approaches for wireless networks. The predefined time slots of S-TDD simplify deployment while restricting its ability to handle changing traffic patterns[4]. D-TDD enhances spectral efficiency along with traffic load adaptability through dynamic time slot allocation based on current traffic requirements[5][6][7]. The main challenge with D-TDD arises from cross-link interference (CLI) which happens when adjacent femtocells or base stations send signals in opposite directions. The distributed evolutionary game-based framework from [8] establishes a method to determine UL/DL subframe allocation for CLI mitigation. The research showed that flexible interference management leads to increased throughput in femtocell networks. The study of [9] proves that cell reconfiguration approaches which consider both inter-cell interference and traffic demands outperform static configurations in mMTC environments where traffic is typically uneven.

2. 5G NR TDD Synchronization

The deployment of 5G New Radio (NR) has driven up the usage of TDD for optimal spectrum utilization especially at mid-band frequencies like 3.5 GHz. The performance of throughput significantly diminishes when neighbouring networks operate without coordination thus requiring TDD cells to be synchronized for minimizing inter-cell interference[10]. The implementation of TDD demands perfect time equality between transmissions to stop collisions whereas FDD operates by separating UL and DL through independent bands. Synchronization signals which include Primary Synchronization Signal (PSS) and Secondary Synchronization Signal (SSS) and 5G Synchronization Signal Block (SSB) perform their main function to synchronize transmissions through accurate frequency and timing references[11]. The research by [12] & [13] shows that adaptive frame structures that balance UL and DL resources together with inter-cell synchronization preservation led to network optimization for uplink-heavy applications. Dense 5G deployments require synchronization to maintain latency performance alongside spectrum efficiency and quality of service.

3. Cross-Link Interference (CLI)

The primary restriction for D-TDD networks exists in CLI which occurs when UL signals between cells disrupt DL signals in another cell or when BS signals from one cell disrupt UL signals in neighbouring cells. The asynchronous UL/DL scheduling between neighbouring cells causes D-TDD networks to generate more CLI interference than S-TDD networks [14]. Research conducted by [15] shows that D-TDD provides better DL throughput than S-TDD however its UL throughput declines because of substantial BS-to-BS interference near the cell perimeter. The interference between links decreases SINR values while simultaneously increasing outage latency times which demands multiple retransmissions that degrade system reliability according to [16]. The dual negative impact of CLI on network throughput and latency demonstrates the critical need for advanced interference reduction solutions in future network systems.

4. Related Works

Several investigations have examined the advantages of D-TDD while working to identify the most efficient methods for reducing interference. The performance of heterogeneous

International Research Journal of Innovations in Engineering and Technology (IRJIET)

ISSN (online): 2581-3048

Volume 9, Issue 8, pp 96-106, August-2025

https://doi.org/10.47001/IRJIET/2025.908013

LTE networks improves through dynamic TDD configuration adaptation yet this approach creates inter-cell interference challenges according to [17]. Contemporary research demonstrates that centralized scheduling approaches combined with beamforming alongside massive MIMO technology provide solutions to reduce interference levels. Research conducted by [18] & [19] demonstrated that inter-site coordination enhances DL and UL performance while coordinated interference cancellation and flexible TDD scheduling lead to uplink throughput gains exceeding 175%. The synchronous D-TDD approach proved to increase both coverage probability and area spectral efficiency according to [20] in their dense small-cell deployment study. Methods based on clustering have been explored for interference mitigation [21] & [22], but their scalability remains limited because of fixed cluster designs that become problematic at boundaries. The combination of stochastic geometry-based models [23] provides both analytical tools for SINR and coverage probability evaluation and improves simulation-based approaches.

Current methods including traditional beamforming and clustering alongside centralized scheduling show potential to minimize D-TDD interference yet they face major obstacles in very dense and heterogeneous environments. A large number of existing methods depend on basic channel representations along with centralized backhaul management and fixed parameters which decreases their flexibility and increases processing delays and system complexity [24] & [25]. The majority of current methods struggle to adapt to real-time traffic changes while also failing to maximize the spatial dimensions of interference. in response to these limitations this study presents an innovative system which integrates distributed resource allocation with real-time interference prediction and adaptive 3D beamforming. The proposed approach works by modifying beam patterns and transmission parameters based on traffic and interference dynamics to significantly minimize CLI which leads to enhanced performance for both DL and UL in D-TDD systems.

III. METHODOLOGY

1. Network Model

The network environment taken into consideration in this study is representative of an ideal cellular system deployment, which is commonly employed to model an actual base station setups and is characterized by a regular hexagonal cell architecture. Each base station is configured with tri-sector antennas to improve directivity and spatial coverage, providing a dependable and organized interference pattern. In an effort to enable flexible switching between uplink and downlink transmission in a shared frequency band, the network implements the dynamic Time Division Duplexing (D-TDD) technique.

Having identified the network environment, we then delve into modeling the network. We start by modelling the network of the system where an ideal tri-sectorial hexagonal network model is considered, with each cell represented by a hexagon and divided into three sectors having a radio site at the center. The hexagonal network is represented byΛ, where b is the number of cell sites and δ is the distance between base station sites. As per the integer coordinates(m, n), each BS site$b_s \in \Lambda$ is indexed such that:

$$b = \delta\left(m + ne^{i\frac{\pi}{3}}\right) \qquad (1)$$

A two-tier heterogeneous network (HetNet) with deployments of macro-cells and small-cells is taken into consideration in this network model. A broad range of network coverage is provided by the macro-cell deployment's implementation of the tri-sectorized hexagonal network structure with multiple base station sites M_b, where the distance between sites is represented by δ. The serving cell is denoted as b_i, such that for each BS, it is assumed that the directional antennas is denoted as$c \in \{1,2,3\}$ which represents the three sectors of the BS antennas and all BSs are of the same height denoted as h_b, with all BS transmitting at the same power level$P$.

In a dynamic-TDD, each BS independently assigns its subframe/slot direction and assuming that the mobility patterns are uniformly distributed and time-dependent, the study examines the environment in which a mobile is serviced by a sector (the first sector) $c = \{1\}$ of the serving cell b_i, with the mobile's location denoted as m_i. As such, the mobility pattern is expresses as:

$$m_i(t) = r(t)e^{i\theta(t)} \qquad (2)$$

Where$r(t)\ and\ \theta(t)$ are time-dependent radial distance and angular position of the user from the serving BS respectively.

2. Dynamic-TDD Model

The Dynamic-TDD networked is then modeled, taking into account its effects on uplink (UL) and downlink (DL) interference, following the establishment of the tri-sectorial hexagonal network. All cells are considered to operate synchronously in either the downlink or the uplink modes when modelling the D-TDD system. The conventional S-TDD systems performance is evaluated utilizing this initial configuration as a benchmark. It is expected that cells will select between uplink and downlink transmission directions in response to high traffic demand since user traffic demands frequently vary. It is assumed that all three sectors at each location have the same transmission direction. As a result, two forms of interference would occur depending on each site's transmission cycle: i) UL to DL Interference: where the cell of interest is in downlink transmission, the uplink signals from

International Research Journal of Innovations in Engineering and Technology (IRJIET)
ISSN (online): 2581-3048
Volume 9, Issue 8, pp 96-106, August-2025
https://doi.org/10.47001/IRJIET/2025.908013

the mobile of the interfering cell interferes with the downlink signal of the cell of interest. ii)DL to UL Interference: where the cell of interest is in uplink transmission, downlink signals from the interfering cell interferes with the signal in uplink of the cell of the serving cell.

By utilizing a full-buffer traffic model, it is assumed that there can be one active transmission (DL or uplink) utilizing a sub-frame on the activation of D-TDD a specific cell. When the D-TDD sub-frame is activated, two Bernoulli Random Variables (RVs) are implemented to indicate the directional probabilities that change dynamically with traffic and time in downlink and uplink in a heterogeneous cellular network (macro-cell and small-cell). These are $\beta_d(b,t)$ and $\beta_u(b,t)$ for the downlink and uplink transmission cycles respectively, such that the density functions of the two RVs are given as:

$$\beta_d(b,t) = \mathbb{P}(\beta_d(b,t)=1)|b \in \Phi_T = a_d^T \quad (3)$$

$$for\ a_d^T \in [0,1]$$

$$\beta_u(b,t) = \mathbb{P}(\beta_u(b,t)=1)|b \in \Phi_T = a_u^T \quad (4)$$

$$for\ a_u^T \in [0,1]$$

$$such\ that\ T \in \{M,S\}$$

3. Pathloss Model

The path loss between transmitter (BS) b and receiver (UE) m is represented as $PL(b,m)$ where the interference in the wireless channels is modelled employing the conventional path-loss model. Therefore, the path-loss between the user equipment and the base station is expressed as:

$$PL(b,m) = a|b-m|^{2b} \quad (5)$$

Where: The path loss between transmitter b and the receiver m is denoted as $PL(b,m)$.The path-loss exponent is denoted as 2b, the path-loss propagation factor is denoted as a, which influences the signal attenuation in diverse environments (i.e. urban and rural), and $|b-m|$ is the average distance between the transmitter b and the receiver m.

In order to keep things simple computationally, the fast-fading model is not used for macro-cell deployment. Instead, link-level performance may reduce the fading impact by changing the SINR to Th. For an Additive Gaussian Noise Channel (AWGN), a modified version of Shannon's formula is used to account for the fast-fading impact, since the connection between (SINR) and (Th) is known. Hence, the following is the expression of Shannon's channel capacity equation:

$$Th = K_1 \log_2(1 + K_2 SINR) \quad (6)$$

The idea of implementing power control is to alter the necessary mobile transmitted power for uplink transmission over the Physical Uplink Shared Channel (PUSCH). Rather of using a preset compensation factor, which only compensates for route loss to some extent, this research makes use of a fractional power control (FPC) factor. Therefore, A mobile device's (receiver's) transmit power to its serving cell's (transmitter's) is defined as:

$$\mathrm{P}_t(b,m) = \mathrm{P}_b(|b-m|^{2b})^k \quad (7)$$

The cell-specific desired power is denoted by P_b, while the power control compensation factor is defined by$k \in [0,0.4,0.8,1]$. The power control technique achieves the target power P_b when $k=1$ by fully compensating for path loss. The path loss is partially adjusted for $0 < k < 1$, which reduces the transmitted power, thereby mitigating mobile user interference at the cell edge. Consequently, for a mobile located at m_i, the power received from the serving BS transmitting with a power level of P can be defined as:

$$\mathrm{P}_r(m_i,b) = \frac{\mathrm{P}G_s(m_i)X(b,m_i)}{L(b,m_i)} \quad (8)$$

4. 3D Beamforming Model

To mitigate CLI, adaptive beam forming can be deployed to dynamically adjust transmission angles in real-time. However, this requires low-latency feedback loops, which may introduce practical deployment challenges. The directional antennas utilized by BSs have a sectorized gain structure. For accurate 3D beam forming simulations, directed radiation patterns are represented for each antenna in both horizontal (H) and vertical (V) planes. 2π-periodic functions are utilized to analytically depict these radiation patterns. Antenna behaviour is characterized and simulated utilizing the Mogensen model as the analytical framework [26] & [27]. The antenna gain is defined utilizing the horizontal and vertical radiation patterns:

$$G_s(m_i) = H(\alpha)V(\phi) \quad (9)$$

$$H(\alpha) = [\cos(\alpha)]^{-2\omega_h} \quad (10)$$

$$V(\phi) = [\cos(\phi)]^{-2\omega_v} \quad (11)$$

Where, ω_h and ω_v are dependent on the horizontal and vertical half-power beamwidth $\theta_{h3dB}\ and\ \theta_{v3dB}(\delta)$ respectively.

5. DL Interference Characterization

In this type of interference, when the serving cell is transmitting in downlink mode, the mobile m_i is impacted by the interference from the downlink operation from the interfering BS and the uplink transmission of the mobiles of the interfering cell. That is, the interference sources are from (i) neighbouring base stations (DL-to-DL) and (ii) uplink mobile transmissions (UL-to-DL).We can define the downlink ISR of a mobile receiver location $\tilde{I}_{DL}(m_i)$ as:

$$\tilde{I}_{DL}(m_i) = \tilde{D}_{dl-dl}(m_i) + \tilde{D}_{ul-dl}(m_i) \quad (12)$$

International Research Journal of Innovations in Engineering and Technology (IRJIET)
ISSN (online): 2581-3048
Volume 9, Issue 8, pp 96-106, August-2025
https://doi.org/10.47001/IRJIET/2025.908013

$\widetilde{D}_{dl-dl}(m_i)$ is defined by the beam forming gains and path-loss models showing the sum of the interfering powers of the neighbouring base stations and $\widetilde{D}_{ul-dl}(m_i)$ as the sum of all the interfering mobiles. Therefore, the interference from the downlink interference sources on the desired DL signal can be expressed as:

$$\widetilde{D}_{dl-dl}(m_i) = \sum_{b_s\in\Lambda} \beta_d(b) G_{DL}(b,m_i) PL(b,m_i) \chi(b,m_i) \quad (13)$$

The uplink interference sources on the desired DL signal can be expressed as:

$$\widetilde{D}_{ul-dl}(m_i) = \sum_{b_s\in\Lambda^*} \beta_u(b) \sum_{c=1}^{3} \frac{\mathrm{P}_t(b)}{PL(m_{i,0},m_i)} \chi(m_{i,0},m_i) \quad (14)$$

The Fenton-Wilkinson technique in [28] is a practical approximation to deal with the sum of log-normal RVs. This involves calculating the mean and the variance to approximate the total of log-normal RVs by a new log-normal RV. Accordingly, (14) becomes dependent on the mobile location m_i and in accordance with the Theorem derived in [29]. The expected values that account for the DL-DL interference is defined as:

$$\mathbb{E}[\widetilde{D}_{dl-dl}(m_i)] = \alpha_d \mathrm{P}_{tb,DL} \lambda_{BS} \sum_{B_s\in\Lambda} \mathbb{E}[G_{DL}(b,m_i)] \mathbb{E}[\chi(b,m_i)] |b-m_i|^{2b} r^{2b} \quad (15)$$

Such that:

$$\mathbb{E}[\chi(b,m_i)] = e^{\frac{\ln(10)^2\sigma^2}{200}} \quad (16)$$

The expression for $\mathbb{E}[G_{DL}(b,m_i)]$ is derived in congruent with [30] which is the expected beam forming gain where the BS uses 3D beam forming and is expressed as:

$$\mathbb{E}[G_{DL}(b,m_i)] = \frac{3\eta V(\phi_{b,c})\Gamma\left(\frac{1}{2}-w_h\right)}{\sqrt{\pi}\Gamma(1-w_h)} \quad (17)$$

Therefore, (15) is further defined as:

$$\mathbb{E}[\widetilde{D}_{dl-dl}(m_i)] = \alpha_d \mathrm{P}_{tb,DL} \lambda_{BS} e^{\frac{\ln(10)^2\sigma^2}{200}} \sum_{B_s\in\Lambda} \mathbb{E}[G_{DL}(b,m_i)] |b-m_i|^{2b} r^{2b} \quad (18)$$

In an effort to determine the uplink to downlink ISR average, the expected values must first be averaged over all of the uplink cells, thereafter, compute an average over both the interfering mobiles' $m_{i,0}$ random positions and the shadowing log-normal RVs, conditional on m. Therefore, (14) becomes:

$$\mathbb{E}[\widetilde{D}_{ul-dl}(m_i)] = \frac{9\alpha_u \mathrm{P}^* \lambda_{UE} e^{\frac{\ln(10)^2\sigma^2}{200}}}{4\pi\delta \mathrm{P}} \sum_{c=1}^{3} \sum_{B_s\in\Lambda^*} \int_0^\infty r^{1+2b(k)+2b} e^{-\frac{r^2}{2\sigma^2}} dr \quad (19)$$

Therefore, by evaluating the radial integral in (19) in closed form, (19) is defined as:

$$\mathbb{E}[\widetilde{D}_{ul-dl}(m_i)] = \frac{9\alpha_u \mathrm{P}^* \lambda_{UE} e^{\frac{\ln(10)^2\sigma^2}{200}}}{4\pi\delta \mathrm{P}} \sum_{c=1}^{3} \sum_{B_s\in\Lambda^*} 2^{b(k+1)} \sigma^{2(1+b(k+1))} \Gamma 1 + b(1+k)) \quad (20)$$

6. UL Interference Characterization

Similar to the characterization of the DL interference, Let$\tilde{I}_{ul}(m_i)$ be the ISR of the serving BS (b_i) and is defined as:

$$\tilde{I}_{ul}(m_i) = \tilde{U}_{ul-ul}(m_i) + \tilde{U}_{dl-ul}(m_i) \quad (21)$$

In the context where the serving cell m_i receives interference from other base stations operating in downlink mode, the downlink to uplink interference $\widetilde{U}_{dl-ul}(m_i)$ is computed by averaging over all downlink-transmitting cells, with respect to the user's location m_i and incorporating the effects of shadow fading and 3D beam forming radiation patterns.As such, the expected value of $\widetilde{U}_{dl-ul}(m_i)$ can is expressed as:

$$\mathbb{E}[\widetilde{U}_{dl-ul}(m_i)] = \alpha_d \mathrm{P}_{tb,DL} \lambda_{BS} \sum_{B_s\in\Lambda^*} \mathbb{E}[G_{DL}(b_i,m)] \mathbb{E}[\chi(b,b_i)] |b-b_i|^{2b} r^{2b(1-k)} \quad (22)$$

By applying the same process as in DL interference and evaluating the mean of the log-normal modeled shadowing, and by dividing the transmit-to-target power ratio, that is the BS transmit power by the UL target power, (22) is further expressed as:

$$\mathbb{E}[\widetilde{U}_{dl-ul}(m_i)] = \frac{\mathrm{P}\alpha_d}{\mathrm{P}^*} \lambda_{BS} e^{\frac{\ln(10)^2\sigma^2}{200}} \sum_{B_s\in\Lambda^*} \mathbb{E}[G_{DL}(b_i,m)] |b-b_i|^{2b} r^{2b(1-k)} \quad (23)$$

International Research Journal of Innovations in Engineering and Technology (IRJIET)

ISSN (online): 2581-3048

Volume 9, Issue 8, pp 96-106, August-2025

https://doi.org/10.47001/IRJIET/2025.908013

The interference which is generated by mobiles (that is uplink to uplink interference) is also accounted for, whereby the neighbouring cell is in uplink transmission, considering that power control model is also applied for the uplink transmission, the expected value for $\tilde{U}_{ul-ul}(m_i)$ is expressed as:

$$\mathbb{E}[\tilde{U}_{ul-ul}(m_i)] = \frac{9}{4\pi\delta} e^{\frac{\ln(10)^2\sigma^2}{200}} \sum_{B_s\in\Lambda} 2^{b(1+k)}\sigma^{2(1+b(1+k))}\Gamma 1 + b(1+k)) \qquad (24)$$

7. SINR and Coverage Probability

The SINR is a downlink and uplink metric that measures the ratio of the received power to the total interference pulse noise at the receiver. Such that:

$$SINR = \frac{P_{rb}}{I+N_0} \qquad (25)$$

By normalizing the signal power P_{rb} such that $P_{rb} = \frac{1}{y_0 r^{2b}}$ and interference power with the thermal noise ηI, the SINR can be expressed as:

$$SINR = \frac{1}{\eta I + \frac{1}{y_0 r^{2b}}} \qquad (26)$$

Coverage probability, which measures the probability that a user (user equipment (UE)) will attain a signal-to-interference-pulse-noise ratio (SINR) greater than a given threshold γ to ensure reliable communication where noise and interference is present, is an essential indicator in evaluating the performance of wireless communication systems, particularly in D-TDD HetNet environments. Where interference is present, the Coverage Probability (γ) (CCDF of SINR) is defined as the probability that a mobile user will be able to attain a SINR threshold in downlink and uplink transmission, such that:

$$P_{cov}(\gamma) = \mathbb{P}[SINR > \gamma] \qquad (27)$$

Therefore, the coverage probability for any user location distribution event is modelled by:

$$P_{cov}(\gamma) = \int_0^\infty \mathbb{P}[SINR > \gamma] f_r(r) dr \qquad (28)$$

IV. RESULTS AND DISCUSSIONS

1. Simulation Parameters

The simulation parameters utilized for the performance analysis are outlined in Table 1.

Table 1: Simulation Parameters

S/N	Parameter	Value
1	Inter-site Distance	1km
2	Antenna gain	17.5dBi
3	BSs height	0.02km
4	Pathloss exponent (2b)	2.5 & 3.5
5	Maximum BS Range	1000m
6	Number of DL/UL Data Symbols	10
7	System Frequency	3.5GHz
8	Modulation Scheme	16QAM
9	Fractional Power Control factor	[0, 0.4, 0.8, 1]

2. Simulation Results

The results displayed in Tables 4.2 and 4.3 provide an in-depth representation of the effectiveness of the enhanced interference mitigation system in both downlink (DL) and uplink (UL) transmissions. Across all values of the fractional power control factor (k), it was found that for the downlink, lower path loss environments (2b = 2.5) consistently achieved higher coverage probability than higher path loss environments (2b = 3.5). For example, the system obtained an index of 0.8631 for 2b = 2.5 at a distance of 100 m from the serving BS and k = 0, as opposed to 0.5725 for 2b = 3.5. Even at full compensation (k = 1), similar performance trends were observed, with narrower beam footprints and higher angular resolution significantly favouring closer users. At the cell edge (900 m), however, the mitigation indices dramatically dropped, highlighting the challenges of suppressing interference at longer ranges where beam footprints grow and angular resolution drops.

The improvement in interference suppression is even more noticeable in the uplink results shown in Table 4.2b. At 100 meters, without power control (k = 0), the system's values were 0.8605 for 2b = 2.5 and 0.5751 for 2b = 3.5. However, when full compensation was applied (k = 1), these values significantly increased to 1.4672 and 0.9806, respectively. Since user transmit powers are typically lower than BS transmit powers, making the system more susceptible to interference variations, this suggests that uplink interference mitigation is more effective than downlink. The trend across distances and k-values showed that environments with lower path loss yielded better performance.

The effectiveness of the improved technique is finally demonstrated by a comparison with the conventional system

International Research Journal of Innovations in Engineering and Technology (IRJIET)

ISSN (online): 2581-3048

Volume 9, Issue 8, pp 96-106, August-2025

https://doi.org/10.47001/IRJIET/2025.908013

(Table 4.3). The improved system demonstrated up to 0.8657 at 2b = 2.5 compared to 0.6982 in the conventional system and 0.5742 at 2b = 3.5 compared to 0.4655 during downlink transmission. In uplink transmission, the improvement was even more prominent. While the conventional system generated 0.9989 at 2b = 2.5 and 0.6659 at 2b = 3.5, the enhanced system achieved noticeably higher indices of 1.4672 and 0.9806, respectively. These results show that the improved system significantly reduces interference and increases coverage probability, particularly in uplink and lower path loss scenarios.

Table 1.2a: Downlink Coverage Result for Conventional System

		3D Beam forming									AVG
Distance from BS (m)		100m	200m	300m	400m	500m	600m	700m	800m	900m	
k=0	2b =2.5	0.696094	0.682031	0.632813	0.527344	0.365625	0.267188	0.189844	0.137109	0.105469	**0.400391**
	2b =3.5	0.464063	0.445313	0.4125	0.3375	0.229688	0.16875	0.117188	0.085313	0.065625	**0.258438**
k=0.4	2b =2.5	0.69679	0.682713	0.633445	0.527871	0.365991	0.267455	0.190034	0.137246	0.105574	**0.400791**
	2b =3.5	0.464527	0.445758	0.412913	0.337838	0.229917	0.168919	0.117305	0.085398	0.065691	**0.258696**
k=0.8	2b =2.5	0.697486	0.683395	0.634078	0.528398	0.366356	0.267722	0.190223	0.137384	0.10568	**0.401191**
	2b =3.5	0.464991	0.446203	0.413325	0.338175	0.230147	0.169088	0.117422	0.085483	0.065756	**0.258954**
k=1	2b =2.5	0.698182	0.684077	0.634711	0.528926	0.366722	0.267989	0.190413	0.137521	0.105785	**0.401592**
	2b =3.5	0.465455	0.446648	0.413738	0.338513	0.230377	0.169256	0.117539	0.085568	0.065822	**0.259213**

Table 2.2b: Uplink Coverage Result for Conventional System

		3D Beam forming									AVG
Distance from BS (m)		100m	200m	300m	400m	500m	600m	700m	800m	900m	
k=0	2b =2.5	0.696094	0.682031	0.625781	0.492188	0.316406	0.175781	0.091406	0.084375	0.077344	**0.360156**
	2b =3.5	0.464063	0.459375	0.43125	0.351563	0.234375	0.13125	0.070313	0.060938	0.051563	**0.250521**
k=0.4	2b =2.5	0.797027	0.780926	0.71652	0.563555	0.362285	0.20127	0.10466	0.096609	0.088559	**0.412379**
	2b =3.5	0.531352	0.525984	0.493781	0.402539	0.268359	0.150281	0.080508	0.069773	0.059039	**0.286846**
k=0.8	2b =2.5	0.897961	0.87982	0.807258	0.634922	0.408164	0.226758	0.117914	0.108844	0.099773	**0.464602**
	2b =3.5	0.598641	0.592594	0.556313	0.453516	0.302344	0.169313	0.090703	0.078609	0.066516	**0.323172**
k=1	2b =2.5	0.998895	0.978715	0.897996	0.706289	0.454043	0.252246	0.131168	0.121078	0.110988	**0.516824**
	2b =3.5	0.66593	0.659203	0.618844	0.504492	0.336328	0.188344	0.100898	0.087445	0.073992	**0.359497**

Table 3.3a: Downlink Coverage Result for Enhanced System

		3D Beam forming									AVG
Distance from BS (m)		100m	200m	300m	400m	500m	600m	700m	800m	900m	
k=0	2b =2.5	0.863114	0.85879	0.83025	0.713496	0.494691	0.361505	0.256859	0.185509	0.142699	**0.52299**
	2b =3.5	0.572527	0.570797	0.544852	0.456638	0.310767	0.228319	0.158555	0.115428	0.088791	**0.338519**
k=0.4	2b =2.5	0.863977	0.859649	0.83108	0.71421	0.495185	0.361866	0.257115	0.185694	0.142842	**0.523513**
	2b =3.5	0.573099	0.571368	0.545396	0.457094	0.311078	0.228547	0.158713	0.115543	0.088879	**0.338858**
k=0.8	2b =2.5	0.86484	0.860507	0.831911	0.714923	0.49568	0.362228	0.257372	0.18588	0.142985	**0.524036**
	2b =3.5	0.573672	0.571938	0.545941	0.457551	0.311389	0.228775	0.158872	0.115659	0.088968	**0.339196**
k=1	2b =2.5	0.865703	0.861366	0.832741	0.715637	0.496175	0.362589	0.257629	0.186066	0.143127	**0.524559**
	2b =3.5	0.574244	0.572509	0.546486	0.458007	0.311699	0.229004	0.15903	0.115774	0.089057	**0.339535**

Table 4.3b: Uplink Coverage Result for Conventional System

		3D Beam forming									AVG
Distance from BS (m)		100m	200m	300m	400m	500m	600m	700m	800m	900m	
k=0	2b =2.5	0.86052	0.851871	0.804305	0.66593	0.428098	0.237832	0.123673	0.114159	0.104646	**0.46567**
	2b =3.5	0.575121	0.57022	0.548888	0.475664	0.317109	0.177581	0.095133	0.082448	0.069764	**0.323548**
k=0.4	2b =2.5	1.062742	1.052061	0.993316	0.822423	0.528701	0.293723	0.152736	0.140987	0.129238	**0.575103**
	2b =3.5	0.710275	0.704222	0.677876	0.587445	0.39163	0.219313	0.117489	0.101824	0.086159	**0.399581**
k=0.8	2b =2.5	1.264964	1.252251	1.182328	0.978917	0.629304	0.349613	0.181799	0.167814	0.15383	**0.684535**
	2b =3.5	0.845428	0.838224	0.806865	0.699226	0.466151	0.261044	0.139845	0.121199	0.102553	**0.475615**
k=1	2b =2.5	1.467186	1.45244	1.371339	1.13541	0.729907	0.405504	0.210862	0.194642	0.178422	**0.793968**
	2b =3.5	0.980581	0.972226	0.935853	0.811007	0.540671	0.302776	0.162201	0.140575	0.118948	**0.551649**

In other to compare the average performance of the two systems, Figures 2, 3, 4 and 5 are plotted from the results in Tables 2 and 3, showing the average coverage performance of the conventional system and enhanced system. Comparing both the enhance system and the conventional system, it is observed that the average interference values where 2b=2.5 is substantially higher than the values where 2b=3.5. Although a high PLE, that is 2b=3.5 will substantially reduce the range and power of interfering signals from distant transmitters, it also limits the coverage area and will require higher transmission power in other to maintain connectivity. With a path-loss exponent (PLE) of 2.5, signals can travel farther and cover a larger area because they attenuate slower over distance. Better signal quality throughout the coverage area ultimately results to augmented coverage probability and more dependable connectivity for subscribers who are farther from the base station [31] & [32].

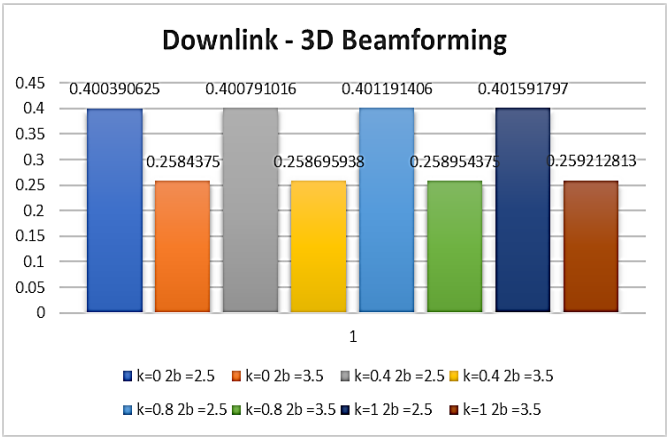

Figure 2: Coverage Probability for Conventional System – Downlink

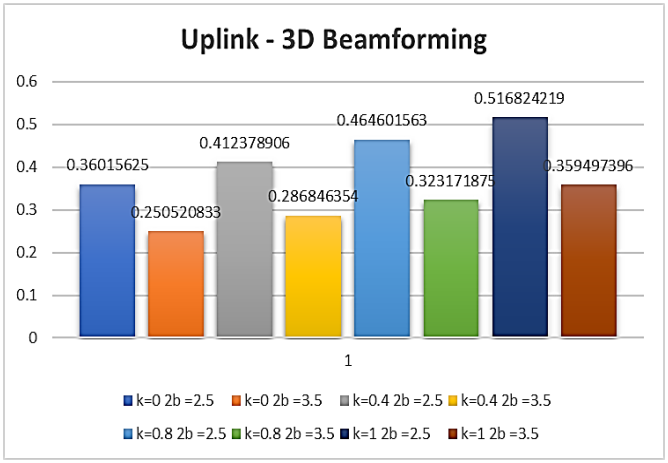

Figure 3: Coverage Probability for Conventional System – Uplink

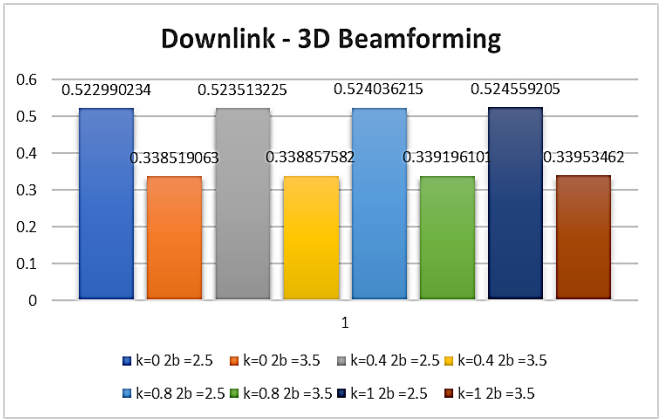

Figure 4: Coverage Probability for Enhanced System – Downlink

International Research Journal of Innovations in Engineering and Technology (IRJIET)

ISSN (online): 2581-3048

Volume 9, Issue 8, pp 96-106, August-2025

https://doi.org/10.47001/IRJIET/2025.908013

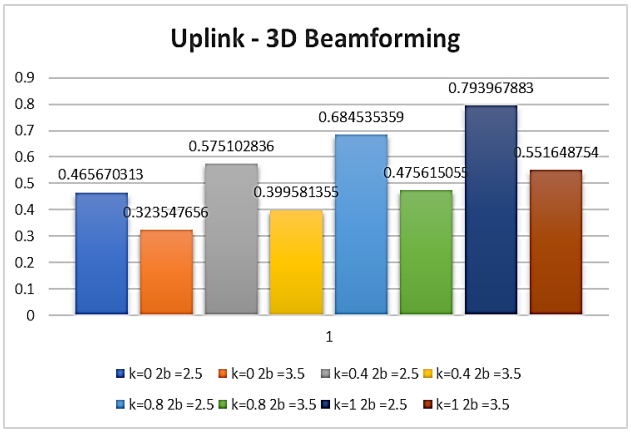

Figure 5: Coverage Probability for Enhanced System – Uplink

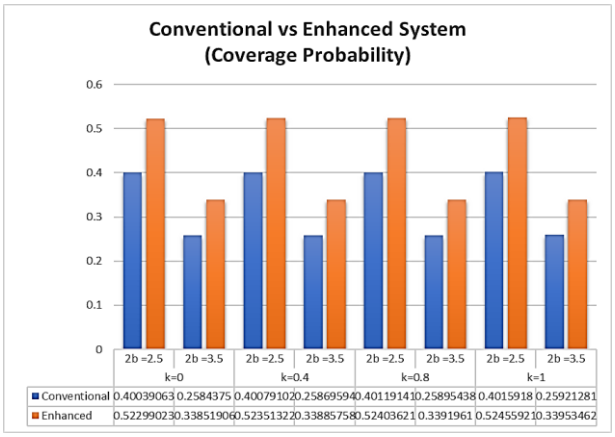

Figure 6: Conventional vs Enhanced System – DL Coverage Probability

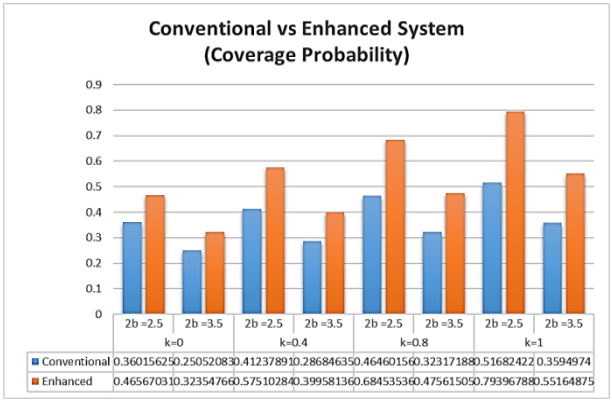

Figure 7: Conventional vs Enhanced System – UL Coverage Probability

3. Average Coverage Probability

The results form tables 4 and 5 shows the coverage percentile difference between the enhanced system and the conventional system during downlink transmission and uplink transmission when 3D beam forming is applied with fractional power control. It is observed that during the downlink transmission, there is over 30% of improvement and up to 53% improvement during the uplink transmission cycle.

Figures 6 and 7 shows that the average mitigation level of the proposed system is over 0.5 during the downlink transmission cycle for all values of FPC, especially 2b = 2.5. During the uplink transmission, the FPC factor of 1 shows a substantial improvement compared to other FPC factor values.

Table 4: Average Downlink Coverage Probability

3D Beam forming		AVG(Conv)	AVG(Enh)	% Improve
k=0	2b =2.5	0.4003906	0.52299	30.62%
	2b =3.5	0.2584375	0.338519	30.99%
k=0.4	2b =2.5	0.400791	0.523513	30.62%
	2b =3.5	0.2586959	0.338858	30.99%
k=0.8	2b =2.5	0.4011914	0.524036	30.62%
	2b =3.5	0.2589544	0.339196	30.99%
k=1	2b =2.5	0.4015918	0.524559	30.62%
	2b =3.5	0.2592128	0.339535	30.99%

Table 5: Average Uplink Coverage Probability

3D Beam forming		AVG(Conv)	AVG(Enh)	% Improve
k=0	2b =2.5	0.3601563	0.46567	29.30%
	2b =3.5	0.2505208	0.323548	29.15%
k=0.4	2b =2.5	0.4123789	0.575103	39.46%
	2b =3.5	0.2868464	0.399581	39.30%
k=0.8	2b =2.5	0.4646016	0.684535	47.34%
	2b =3.5	0.3231719	0.475615	47.17%
k=1	2b =2.5	0.5168242	0.793968	53.62%
	2b =3.5	0.3594974	0.551649	53.45%

4. Discussion of Findings

The results presented in the preceding subsections show that by enabling each base station (BS) to dynamically switch between downlink (DL) and uplink (UL) transmissions based on the current traffic demand, Dynamic Time Division Duplexing (D-TDD) can significantly minimize the interference between adjacent cells. The fixed frame structure of Static TDD (S-TDD), in which every cell utilizes a set DL/UL configuration irrespective of traffic asymmetry, stands in contrast to this flexibility. D-TDD improves the throughput performance and coverage probability by allowing user-centric scheduling of DL and UL transmissions. This ensures that transmission resources are distributed in a way that minimizes strong cross-link interference (CLI). The developed model makes use of adaptive transmission decisions, which lead to the alignment of interference between cells of interest, contrary to the S-TDD configurations. This minimizes the likelihood of UL-to-DL interference, which occurs when an uplink user in the adjacent cell interferes with a downlink user in the cell of interest, and the DL-to-UL interference, which occurs when a macro-cell or small-cell of the adjacent cell transmitting in downlink interferes with the uplink received signal of the cell of interest. Due to the fact that the cell-edge users are more susceptible to weaker signal strengths, such interference situations are especially harmful to them. The model makes sure that desired users have less signal quality

ISSN (online): 2581-3048
Volume 9, Issue 8, pp 96-106, August-2025
https://doi.org/10.47001/IRJIET/2025.908013

degradation by focusing the intended beams and resources on them at specific times, which increases network fairness.

The network coverage probability significantly improves when the system functions with Dynamic TDD compared to Static TDD across various path loss exponents and fractional power control settings, as shown in figures 6 and 7. The adaptive nature of D-TDD enables cells to optimize their transmission directions between uplink and downlink operations depending on channel performance metrics and immediate traffic requirements which leads to this enhanced performance. Cross-link interference is severe in the heterogeneous deployments that include both small and macro cells in S-TDD configuration, where all cells have fixed DL/UL transmission patterns. It is observed in table 2 that there is significant improvement in coverage of 30% in downlink transmission and 53% in uplink transmission from table 3.

These findings further demonstrate a significant asymmetry in the characteristics of interference: the interference on uplink users (DL-to-UL interference) is more severe when the interferer is a base station transmitting in the DL compared to when the interferer is a mobile device transmitting in the UL (UL-to-DL interference). DL-to-UL interference is a more prevalent impairment in D-TDD networks, which is explained by the fact that base stations have a higher transmit power than mobile devices. By carefully coordinating DL and UL transmissions between cells, the proposed model minimizes the likelihood of the interference overlap.

V. CONCLUSION

The research evaluated the enhanced D-TDD interference mitigation framework through adaptive 3D beamforming and fractional power control in heterogeneous cellular networks. The analytical models for ISR, SINR and coverage probability helped to measure the performance of the proposed system against conventional S-TDD and D-TDD across different path loss conditions and fractional power control settings. The enhanced system demonstrated continuous coverage probability enhancement for both uplink and downlink operations reaching average gains of 30% for downlink and 53% for uplink transmissions. The performance benefits become more substantial when operating in low path loss environments (2b = 2.5) because the system can achieve better interference suppression through narrower beam footprints combined with higher angular resolution. The research shows that CLI interference from DL transmissions to UL transmissions produces more performance degradation than UL to DL interference because base stations operate with greater transmission power levels than mobile devices. The proposed system reduces interference imbalances by dynamically adjusting transmission directions and applying interference-aware beamforming which delivers enhanced coverage reliability for users at all network locations. The improved system demonstrates better interference management and resource optimization than traditional systems which proves its suitability for dense 5G networks and future wireless deployments. The research shows that combining dynamic interference-aware beamforming with real-time traffic adaptation enables scalable and reliable interference management for next-generation wireless networks.

REFERENCES

[1] Parkvall, S., Dahlman, E., Furuskar, A., & Frenne, M. (2017). NR: The new 5G radio access technology. *IEEE Communications Standards Magazine*, 1(4), 24-30.

[2] Dahlman, E., Parkvall, S., & Skold, J. (2020). 5G NR: The next generation wireless access technology. *Academic Press*.

[3] 3GPP. (2017, February-c). Discussion on duplexing flexibility and cross-link interference mitigation schemes (3GPP TSG RAN WG1 Meeting #88, R1-1701616, Issue. https://www.3gpp.org/

[4] WrayCastle. (2024). Time Division Duplexing Explained: A Beginner's Guide to Efficient Communication. https://wraycastle.com/blogs/knowledge-base/what-is-time-division-duplexing.

[5] Zhu, D., & Lei, M. (2013a). Cluster-based dynamic DL/UL reconfiguration method in centralized RAN TDD with dense deployment of remote radio units. *2013 IEEE 77th Vehicular Technology Conference (VTC Spring).*

[6] Sun, F., & Zhao, Y. (2016). Cell cluster-based dynamic TDD DL/UL reconfiguration in TD-LTE systems *2016 IEEE Wireless Communications and Networking Conference.*

[7] Ji, H., Kim, Y., Choi, S., Cho, J., & Lee, J. (2013). Dynamic resource adaptation in beyond LTE-A TDD heterogeneous networks. *2013 IEEE International Conference on Communications Workshops (ICC).*

[8] Chao, C.-C., Lee, C.-H., Wei, H.-Y., Wang, C.-Y., & Chen, W.-T. (2015). Distributed dynamic-TDD resource allocation in femtocell networks using evolutionary game *2015 IEEE 26th Annual International Symposium on Personal, Indoor, and Mobile Radio Communications (PIMRC)*.

[9] Ardah, K., Fodor, G., Silva, Y. C., Freitas, W. C., & Cavalcanti, F. R. (2017). A novel cell reconfiguration technique for dynamic TDD wireless networks. *IEEE Wireless Communications Letters*, 7(3), 320-323.

[10] ECC, R. (2019). National synchronisation regulatory framework options in 3400-3800 MHz: a toolbox for

ISSN (online): 2581-3048
Volume 9, Issue 8, pp 96-106, August-2025
https://doi.org/10.47001/IRJIET/2025.908013

coexistence of MFCNs in synchronized, unsynchronized and semi-synchronized operation in 3400-3800 MHz. https://www.scribd.com/document/552265275/ECC-Report-296.

[11] KP. (2019). 5G NR: Secondary Synchronization Signal (SSS). https://howltestuffworks.blogspot.com/2019/10/5g-nr-secondary-synchronization-signal.html.

[12] Ruffini, S., Johansson, M., Pohlman, B., & Sandgren, M. (2021). 5G synchronization requirements and solutions. *Ericsson technology review*, 2021(1), 2-13.

[13] GSMA. (2020). TDD Synchronization at the 3.5GHz range – a key step for 5G success. https://www.gsma.com/spectrum/resources/3-5-ghz-5g-tddsynchronisation/.

[14] Kulkarni, M. N., Andrews, J. G., & Ghosh, A. (2017). Performance of Dynamic and Static TDD in Self-Backhauled Millimeter Wave Cellular Networks. *IEEE Transactions on Wireless Communications*, 16(10), 6460-6478. https://doi.org/10.1109/twc.2017.2723887.

[15] Yang, H. H., Geraci, G., Zhong, Y., & Quek, T. Q. S. (2017). Packet Throughput Analysis of Static and Dynamic TDD in Small Cell Networks. *IEEE Wireless Communications Letters*, 6(6), 742-745. https://doi.org/10.1109/lwc.2017.2738019.

[16] Yassin, M., Dirani, Y., Ibrahim, M., Lahoud, S., Mezher, D., & Cousin, B. (2015). A novel dynamic inter-cell interference coordination technique for LTE networks *2015 IEEE 26th Annual International Symposium on Personal, Indoor, and Mobile Radio Communications (PIMRC)*.

[17] Khoryaev, A., Chervyakov, A., Shilov, M., Panteleev, S., & Lomayev, A. (2012). Performance analysis of dynamic adjustment of TDD uplink-downlink configurations in outdoor picocell LTE networks. *2012 IV International Congress on Ultra-Modern Telecommunications and Control Systems.*

[18] Lukowa, A., & Venkatasubramanian, V. (2016). Performance of strong interference cancellation in flexible UL/DL TDD systems using coordinated muting, scheduling and rate allocation *2016 IEEE Wireless Communications and Networking Conference.*

[19] Lukowa, A., & Venkatasubramanian, V. (2018). On the Performance of 5G Flexible TDD Systems with Coordinated Beamforming *2018 14th International Conference on Wireless and Mobile Computing, Networking and Communications (WiMob).*

[20] Ding, T., Ding, M., Mao, G., Lin, Z., Zomaya, A. Y., & Lopez-Perez, D. (2018). Performance Analysis of Dense Small Cell Networks With Dynamic TDD. *IEEE Transactions on Vehicular Technology*, 67(10), 9816-9830. https://doi.org/10.1109/tvt.2018.2854287.

[21] Gao, Y., Cheng, L., Li, Y., Zhang, X., & Yang, D. (2015). Performance Evaluation on Cell Clustering Interference Mitigation and CoMP in Multi-Pico Network with Dynamic TDD *2015 IEEE 81st Vehicular Technology Conference (VTC Spring).*

[22] Lin, Y.-T., Chao, C.-C., & Wei, H.-Y. (2015). Dynamic TDD interference mitigation by using soft reconfiguration. *2015 11th international conference on heterogeneous networking for quality, reliability, security and robustness (QSHINE).*

[23] Andrews, J. G., Baccelli, F., & Ganti, R. K. (2011). A Tractable Approach to Coverage and Rate in Cellular Networks. IEEE Transactions on Communications, 59(11), 3122-3134. https://doi.org/10.1109/tcomm.2011.100411.100541.

[24] Lukowa, A., &Venkatasubramanian, V. (2019). Centralized UL/DL Resource Allocation for Flexible TDD Systems with Interference Cancellation. *IEEE Transactions on Vehicular Technology*, 68(3), 2443-2458. https://doi.org/10.1109/tvt.2019.2893061.

[25] Tan, J.-S., Yang, S., Meng, K., Zhang, J., Tang, Y., Bu, Y., & Wang, G. (2023). Lightweight machine learning for digital cross-link interference cancellation with RF chain characteristics in flexible duplex MIMO systems. *IEEE Wireless Communications Letters*, 12(7), 1269-1273.

[26] Mogensen, P. E., Pedersen, K. I., Leth-Espensen, P., Fleury, B., Frederiksen, F., Olesen, K., & Larsen, S. L. (1997). Preliminary measurement results from an adaptive antenna array testbed for GSM/UMTS. *1997 IEEE 47th Vehicular Technology Conference. Technology in Motion.*

[27] Rachad, J., Nasri, R., & Decreusefond, L. (2019). A 3D beamforming scheme based on the spatial distribution of user locations. *2019 IEEE 30th Annual International Symposium on Personal, Indoor and Mobile Radio Communications (PIMRC).*

[28] Fenton, L. (1960). The sum of log-normal probability distributions in scatter transmission systems. *IRE Transactions on communications systems*, 8(1), 57-67.

[29] Jacod, J., & Protter, P. (2012). Probability essentials. *Springer Science & Business Media*.

[30] Rachad, J., Nasri, R., & Decreusefond, L. (2019). A 3D beamforming scheme based on the spatial distribution of user locations. *2019 IEEE 30th Annual International Symposium on Personal, Indoor and Mobile Radio Communications (PIMRC).*

[31] Alex, A., Aliou, B., Aladji, K., Adama, K., Tabbabi, O., & Olivier, A. (2021). Measurements Based Evaluation of Pathloss Exponenets in Urban Outdoor Environments. *International Journal of Advanced Research (IJAR)*, 9(03), 72-79. https://doi.org/10.21474/IJAR01/12556.

ISSN (online): 2581-3048
Volume 9, Issue 8, pp 96-106, August-2025
https://doi.org/10.47001/IRJIET/2025.908013

[32] Razali, N. A. M., Habaebi, M. H., Zulkurnain, N., Islam, M. R., & Zyoud, A. (2017). The distribution of path loss exponent in 3D indoor environment. *Int. J. Appl. Eng. Res*, 12(18), 7154-7161.

Citation of this Article:

Praise Igochi Onu, & Bourdillon O. Omijeh. (2025). Adaptive Uplink-Downlink Resource Partitioning for CLI Mitigation in 5G HetNets with Dynamic-TDD. *International Research Journal of Innovations in Engineering and Technology - IRJIET*, 9(8), 96-106. Article DOI https://doi.org/10.47001/IRJIET/2025.908013

****

